The EMBO Journal Vol.17 No.8 pp.2392–2403, 1998

Dissecting RNA recombination *in vitro*: role of RNA sequences and the viral replicase

Peter D.Nagy[1], Chunxia Zhang[1,2] and Anne E.Simon[1,2,3]

[1]Department of Biochemistry and Molecular Biology and [2]Program in Molecular and Cellular Biology, University of Massachusetts, Amherst, MA 01003, USA

[3]Corresponding author

Molecular mechanisms of RNA recombination were studied in turnip crinkle carmovirus (TCV), which has a uniquely high recombination frequency and non-random crossover site distribution among the recombining TCV-associated satellite RNAs. To test the previously proposed replicase-driven template-switching mechanism for recombination, a partially purified TCV replicase preparation (RdRp) was programed with RNAs resembling the putative *in vivo* recombination intermediates. Analysis of the *in vitro* RdRp products revealed efficient generation of 3′-terminal extension products. Initiation of 3′-terminal extension occurred at or close to the base of a hairpin that was a recombination hotspot *in vivo*. Efficient generation of the 3′-terminal extension products depended on two factors: (i) a hairpin structure in the acceptor RNA region and (ii) a short base-paired region formed between the acceptor RNA and the nascent RNA synthesized from the donor RNA template. The hairpin structure bound to the RdRp, and thus is probably involved in its recruitment. The probable role of the base-paired region is to hold the 3′ terminus near the RdRp bound to the hairpin structure to facilitate 3′-terminal extension. These regions were also required for *in vivo* RNA recombination between TCV-associated sat-RNA C and sat-RNA D, giving crucial and direct support for a replicase-driven template-switching mechanism of RNA recombination.

Keywords: plant virus/recombination/replication/satellite RNA/template switching

Introduction

Genetic RNA recombination is a process that joins together two non-contiguous RNA segments (King, 1988; Lai, 1992). The term currently is used only for RNA molecules that carry genomic functions (i.e. genomes of RNA viruses, satellites and viroids), thereby excluding RNA processing, splicing and editing. RNA recombination is well documented for a large number of viruses, and is believed to have affected viral evolution and adaptation (King, 1988; Strauss and Strauss, 1988; Lai, 1992; Dolja and Carrington, 1992; Simon and Bujarski, 1994). Recent studies on RNA recombination with RNA viruses revealed roles for RNA recombination in creating novel chimeric viruses, recovering functional genomes from mutated (damaged) RNAs and contributing to the quasispecies nature of RNA viruses (Zimmern, 1988; Lai, 1992; Nagy and Bujarski, 1996; Simon and Nagy, 1996). RNA recombination is also a risk factor in some transgenic systems by facilitating the generation of unwanted viral recombinants (Greene and Allison, 1994).

Early studies on RNA recombination suggested an infrequent occurrence and a scattered distribution of junction sites (Kirkegaard and Baltimore, 1986; King, 1988). These features and the existence of strong selection pressure favoring only the accumulation of viable recombinants made studies on the molecular mechanisms of RNA recombination difficult. However, comparison of RNA recombinants isolated in numerous viral systems led to the classification of recombinants as homologous or non-homologous (King, 1988; Lai, 1992). The former recombinants were those that were generated from two homologous RNAs and had junction sites located within similar sequences, while the latter were derived from two dissimilar RNAs.

Recent development of site- (or short region-) specific, targeted RNA recombination systems for brome mosaic bromovirus (BMV), tomato bushy stunt tombusvirus and turnip crinkle carmovirus (TCV) allowed further refinement of the RNA determinants and molecular mechanisms of RNA recombination (reviewed by Nagy and Simon, 1997). For the tricomponent BMV, inserting a short RNA1-derived sequence into an RNA3 derivative in the complementary orientation induced the generation of non-homologous RNA1–RNA3 recombinants (Nagy and Bujarski, 1993). In addition, insertion of a short RNA2-derived region in the direct orientation into an RNA3 derivative facilitated RNA2–RNA3 crossovers that were of the homologous type, since the junctions were located precisely within the common regions (Nagy and Bujarski, 1995). A replicase-driven template-switching mechanism for both homologous and non-homologous recombination was supported by the distribution of recombinant junctions on the RNAs and the observation that mutations within the two virus-encoded components of the replicase influenced the frequency of recombinant accumulation and the distribution of junction sites (Nagy and Bujarski, 1993, 1997; Nagy *et al.*, 1995; Figlerowitz *et al.*, 1997). Using chimeric tombusviruses, White and Morris (1995) found that preferred junction sites were the 5′ termini and strong hairpin structures in the donor templates. Hairpin structures that were proposed to facilitate the re-initiation of RNA synthesis during the template-switching events were also involved in generating TCV recombinants (Cascone *et al.*, 1990, 1993; Carpenter *et al.*, 1995).

TCV is a 4054 base RNA virus that uniquely is associated with a number of subviral RNAs, including satellite, defective-interfering and chimeric RNAs (Simon

and Nagy, 1996). RNA species in the latter two groups are the products of natural recombination. For example, the chimeric sat-RNA C (356 nucleotides) is composed of sequences similar to a satellite RNA (sat-RNA D, 194 nucleotides) at its 5′ end and two 3′-proximal regions from TCV genomic RNA at its 3′ end (Simon and Howell, 1986). High frequency recombination was observed *in vivo* between sat-RNA D and sat-RNA C, with the recombination junctions clustered close to or at the 3′ end of sat-RNA D and at the base of a hairpin (designated motif1-hairpin) in the center portion of sat-RNA C (Cascone *et al.*, 1990, 1993). Non-compensatory mutations in the stem of the motif1-hairpin eliminated detectable recombinants *in vivo*. In addition, part of the sequence of the motif1-hairpin contains similarity with the 5′-end region of the TCV genomic RNA that probably contains the promoter for positive strand synthesis. These results suggested that the motif1-hairpin is involved in recruitment of the RdRp during re-initiation of synthesis following the template switch. The model predicted that the viral replicase (RNA-dependent RNA polymerase, RdRp) uses the nascent, positive-stranded sat-RNA D as a primer to resume RNA elongation on the acceptor sat-RNA C template during the recombination events (Cascone *et al.*, 1993; Simon and Nagy, 1996).

The replicase-mediated template-switching models suggest that recombination can be divided into three steps: (i) generation of the primer on the donor RNA; (ii) strand transfer and the binding of the RdRp to the acceptor RNA; and (iii) primer elongation on the acceptor RNA (Jarvis and Kirkegaard, 1991; Lai, 1992; Nagy and Simon, 1997). In this report, two questions relevant to the strand transfer and primer elongation steps have been studied: (i) how a promoter-dependent RdRp, such as the TCV RdRp, associates with the acceptor RNAs and (ii) how the RdRp is capable of primer extension, a process fundamentally different from *de novo* initiation. We report the development of a cell-free (*in vitro*) system that uses hybrid RNAs that resembled putative recombination intermediates to program partially purified TCV RdRp preparations. These hybrid RNAs supported 3′-terminal extension (3′-TX), which is analogous to primer extension proposed to occur *in vivo* by the TCV RdRp (Cascone *et al.*, 1993; Simon and Nagy, 1996). Comparison of the *in vitro* and *in vivo* results demonstrates that the *in vitro* system can faithfully copy most of the aspects of the *in vivo* system, giving direct support for a replicase-driven template-switching mechanism for RNA recombination.

Results

Development of an in vitro system to study RNA recombination

The TCV RdRp, similarly to many other viral RdRps, replicates the TCV genomic RNA and all the associated RNAs by recognizing specific promoter sequences/structures present on these RNAs and initiating RNA synthesis *de novo* (Song and Simon, 1994, 1995; Guan *et al.*, 1997). In addition, the TCV RdRp is capable of primer elongation, but only from the 3′ end of the plus strand and only in the presence of a functional promoter (i.e. the TCV RdRp was unable to extend primers hybridizing randomly at internal positions) (Nagy *et al.*, 1997; C.Song and A.E. Simon, unpublished). However, according to the model of RNA recombination in TCV, the RdRp must be able to extend on the nascent strand at internal positions on the template RNA using the nascent RNA strand as a primer during the crossover events. To determine whether the TCV RdRp is capable of primer extension when supplied with putative recombination intermediates, we have used an *in vitro* system that includes the putative recombination intermediates of a previously defined RNA recombination system between sat-RNA C and sat-RNA D: the negative-stranded sat-RNA C, TCV RdRp, and positive-stranded, nearly full-length nascent strand of sat-RNA D (Figure 1A). The model also predicts that the nascent positive strand of sat-RNA D is used by the TCV RdRp as a primer to extend RNA synthesis on the acceptor sat-RNA C from the base of the motif1-hairpin (Cascone *et al.*, 1990). Sequence comparison of junction regions revealed complementarity between the 3′-end region of the nascent sat-RNA D positive strand and a region 3′ of the motif1-hairpin in the negative strand of sat-RNA C (Figure 1A), with the sequences predicted to form a stable base-paired structure (priming stem).

The cell-free (*in vitro*) system makes use of a partially purified, template-dependent TCV RdRp preparation (Song and Simon, 1994). The TCV RdRp preparation was programed with RNA templates that were designed to resemble the above-described putative recombination intermediates (Figure 1B). One of these constructs, designated CD-13mini, consisted of sequences corresponding to the central portion of the negative strand of sat-RNA C (total of 84 nucleotides, including the *in vivo* recombination hotspot region and the motif1-hairpin, plus short 5′- and 3′-flanking sequences) and a 28 nucleotide segment of the positive-stranded sat-RNA D with the 3′ terminus representing the *in vivo* recombination hotspot position –13 (relative to the 3′ end) (Figure 1B). This hybrid construct was designed to avoid known transcriptional promoters in sat-RNA C minus strands and sat-RNA D plus strands. A six-nucleotide artificial loop sequence was used to covalently link the sat-RNA D plus strand fragment to the sat-RNA C minus strand fragment, as depicted in Figure 1B, to ensure that an optimal 1:1 molar ratio of interacting sequences were in proximity and in the correct orientation. If the model for recombination between sat-RNAs D and C is correct, then the TCV RdRp should start 3′-TX, analogously to recombination *in vivo*, at the base of the motif1-hairpin in the hybrid construct (Figure 1C). This ‘self-primed’ 3′-TX reaction is expected to generate a product that has a hairpin-like structure with a long double-stranded region and short loop sequence (schematically shown in Figure 1C).

The major 3′-TX product generated using CD-13mini template in the RdRp reaction migrated faster than the 117 nucleotide full-length input RNA in denaturing polyacrylamide gels, as expected for a hairpin-like RNA molecule possessing an extremely stable secondary structure. Treatment of the 3′-TX product with single strand-specific S1 nuclease resulted in degradation of the 3′-TX product into two new radiolabeled RNA species, one migrating at a position of ~80 nucleotides, and the second at ~65 nucleotides (Figure 1D). The occurrence of two S1 nuclease-resistant products is probably due to partial digestion at the mismatched region in the priming stem

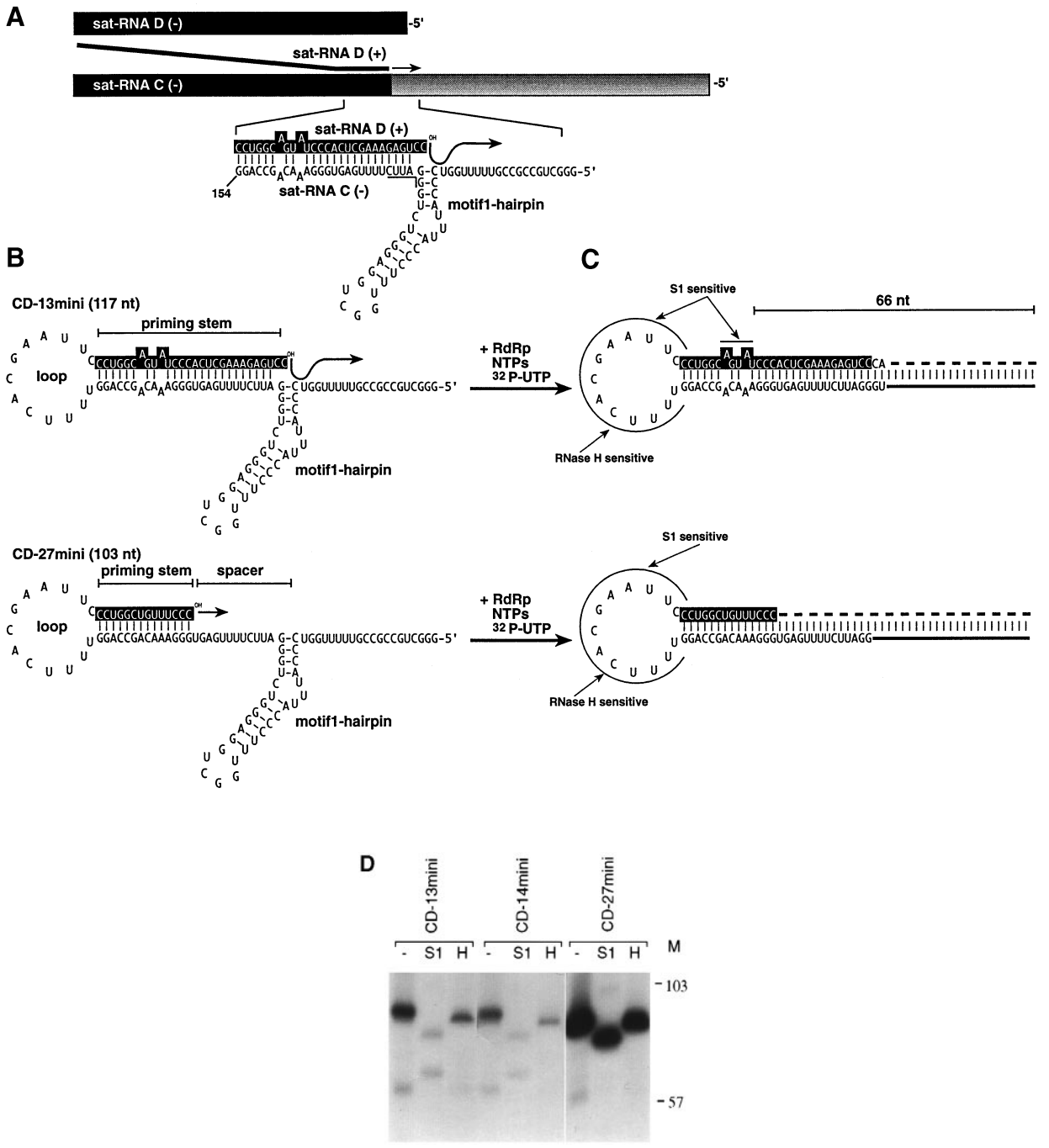

Fig. 1. An *in vitro* system to study RNA recombination in TCV. (**A**) The *in vivo* system. Model for RNA recombination between sat-RNA D and sat-RNA C by a replicase-driven template-switching mechanism. The recombination intermediates are depicted, showing the possible RNA–RNA interaction between the nascent sat-RNA D plus strand, truncated at position –13 at the 3′ end (in *in vivo* experiments, the junctions were located most frequently at positions –13 to –15, as counted from the 3′ end), and sequence 3′ of the motif1-hairpin of sat-RNA C minus strand (the acceptor RNA strand). Sat-RNA D sequence is boxed in black. Underlined nucleotides at the base of the motif1-hairpin indicate the location of the *in vivo* junction site hotspot in sat-RNA C. In the rectangles representing the sat-RNAs, similar regions are shaded alike. (**B**) *In vitro* system that mimics the putative *in vivo* recombination intermediate. Top construct (CD-13mini) contains 28 nucleotides from sat-RNA D plus strand (boxed in black), extending from position –13 at the 3′ end, joined by a six-base artificial sequence (5′-GAAUUC-3′) to sat-RNA C minus strand sequence that includes 33 nucleotides 3′ of the motif1-hairpin, the motif1-hairpin, and 18 nucleotides 5′ of the hairpin (plus two non-viral G residues at the 5′ end). Bottom construct (CD-27mini), same as CD-13mini except that the sat-RNA D sequence terminates at the –27 position and two mismatches in the priming stem are mutated such that base pairing can occur throughout the priming stem. Regions referred to in the text as the priming stem, motif1-hairpin, loop and spacer are shown. (**C**) Products of the primer extension reactions (3′-TX). Addition of partially purified TCV RdRp, ribonucleotides and radioactive UTP results in an intramolecular extension from the 3′-terminal sat-RNA D sequence for CD-13mini and CD-27mini using sat-RNA C sequence as template. The radiolabeled portion of the product is shown by a thick dotted line. S1 nuclease-sensitive and RNase H-sensitive (following hybridization of loop1 oligo DNA to the loop region, depicted by a solid line) sites are indicated. (**D**) Efficient 3′-TX by the TCV RdRp. Denaturing gel analysis of radiolabeled 3′-TX products synthesized by *in vitro* transcription with TCV RdRp. Lanes depicted by –, S1 and H denote products that were untreated, or treated with either S1 nuclease or RNase H, respectively. M, single-stranded RNA markers (in bases). The template RNAs were CD-13mini (B), CD-14mini (one base 3′-end truncation derivative of CD-13mini) and CD-27mini (B). Note that in the untreated samples, the hairpin-like RNAs migrate aberrantly, much faster than their corresponding sizes in denaturing gels.

of CD-13mini resulting in a shorter, ~65 nucleotide product, and more complete digestion in the single-stranded loop giving the ~80 nucleotide product (Figure 1C). Specific digestion of the loop region of the 3′-TX products obtained with CD-13mini template by RNase H in the presence of an oligodeoxyribonucleotide (loop1 oligo, complementary to the loop region of CD-13mini) (Figure 1C) resulted in a single radiolabeled RNA product migrating at a position of ~85 nucleotides (Figure 1D). In combination with the S1 analysis, the data indicate that initiation of 3′-TX occurred at the base of the motif1-hairpin on the CD-13mini template (schematically shown in Figure 1C).

To investigate the role of the sat-RNA D-derived region in 3′-TX reactions, deletion of one base and 14 bases were made from the 3′ end of CD-13mini (Figure 1B), generating CD-14mini (not shown) and CD-27mini (Figure 1B), respectively, which contain 3′ ends corresponding to the –14 and –27 positions of sat-RNA D. While the –14 position was a frequent junction in *in vivo* recombinants, the –27 position has never been found (Cascone *et al.*, 1990, 1993; Carpenter *et al.*, 1995). In addition, CD-27mini contained two mutations that allowed for complete hybridization between sat-RNA D and the region 3′ of the sat-RNA C motif1-hairpin (Figure 1B). CD-14mini and CD-27mini generated the hairpin-sized 3′-TX products that migrated similarly to the 3′-TX product obtained with CD-13mini (Figure 1D). The sizes of the S1 nuclease-digested products were also similar for CD-13mini and CD-14mini, while CD-27mini had only a single S1 nuclease-resistant product that co-migrated with the ~80 nucleotide product for CD-13mini (Figure 1D). The existence of a single S1 nuclease-resistant radiolabeled 3′-TX product for CD-27mini was consistent with the lack of mismatched bases in the primer stem region of CD-27mini eliminating the S1 nuclease-sensitive site present in CD-13mini and CD-14mini. Since CD-13mini, CD-14mini and CD-27mini generated single RNase H-resistant radiolabeled products of similar size, 3′-TX for CD-14mini and CD-27mini must have initiated ~1 and ~13 nucleotides, respectively, 3′ of the initiation site for CD-13mini, which was at the base of the motif1-hairpin. Quantitation of the 3′-TX products by densitometric scanning of exposed films followed by normalization for the number of adenylate residues on the template portion of the respective RNA revealed that CD-14mini was 27.9 ± 2.3% less active in generating hairpin-sized 3′-TX products when compared with CD-13mini. Surprisingly, CD-27mini was ~6-fold (603.3 ± 39.5%) more active than CD-13mini (100%) in the 3′-TX reactions. The elevated activity of CD-27mini was probably due to a spacer region (see Figure 1B) located between the priming stem and motif1-hairpin and not the mutations that eliminated the mismatched bases from the priming stem, since introduction of two similar mutations to the priming stem of CD-27mini did not reduce the level of 3′-TX (data not shown). This CD-27mini with a mutated priming stem generated 3′-TX products that resulted in two radiolabeled RNA species following S1 nuclease treatment, which co-migrated with those obtained with CD-13mini (data not shown).

The motif1-hairpin is required for high level 3′-TX in vitro

One of the hallmarks of recombination between sat-RNA C and sat-RNA D is the requirement for the motif1-hairpin

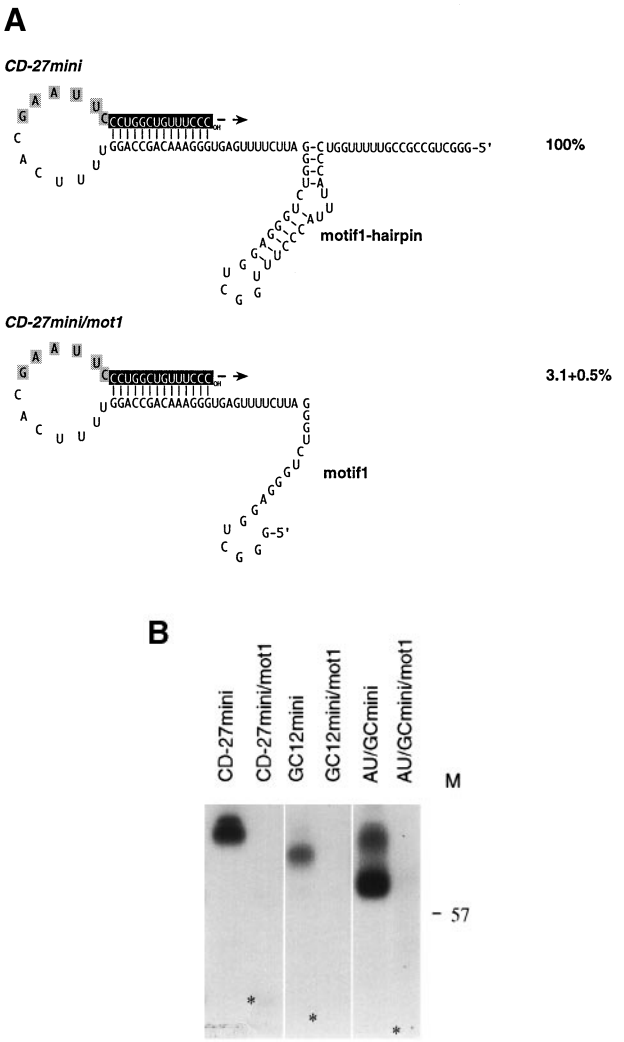

Fig. 2. The motif1-hairpin facilitates 3′-TX. (**A**) Sequences and structures of CD-27mini, CD-27mini/mot1, which lacks the 5′ end sequence, and the 5′ portion of the motif1-hairpin. The efficiency of 3′-TX was analyzed by denaturing PAGE, followed by autoradiography and densitometry. The data were normalized based on the amount of template-directed radioactive UTP incorporated. The standard error was calculated from three separate experiments. (**B**) A representative experiment showing denaturing gel analysis of radiolabeled and S1-treated 3′-TX products synthesized by *in vitro* transcription with TCV RdRp using CD-27mini, CD-27mini/mot1, GC12mini, GC12mini/mot1, AU/GCmini and AU/GCmini/mot1 (see Figure 5) as templates. M, single-stranded RNA markers (in bases).

sequence and/or structure *in vivo* (Cascone *et al.*, 1990, 1993; reviewed by Simon and Nagy, 1996). To test for involvement of the motif1-hairpin in the 3′-TX with our chimeric constructs *in vitro*, CD-27mini/mot1, which contained only the 3′-half of the motif1-hairpin and the priming stem, was constructed (Figure 2A). The 3′-TX product for CD-27mini/mot1 was reduced by ~30-fold from the level obtained using CD-27mini (Figure 2B). This result demonstrates that the priming stem alone cannot support efficient 3′-TX and that the motif1-hairpin is required for efficient 3′-TX from the priming stem *in vitro*. Thus, as predicted by the RdRp-mediated template-switching model of recombination, 3′-TX (and possibly the analogous *in vivo* recombination reaction) is a more complex phenomenon than a simple primer extension reaction (see Discussion). In addition, the requirement for

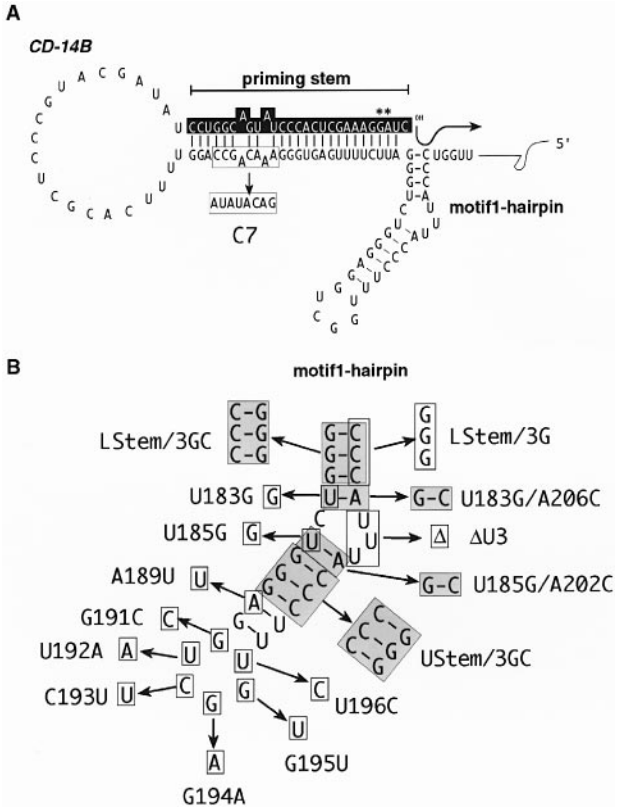

Fig. 3. Mutations in the motif1-hairpin influence 3′-TX. (**A**) Sequence and structure of the basic CD-14B construct. Shadings are as described in the legend to Figure 1. Asterisks denote the positions of base alterations from CD-13mini (Figure 1B) to generate a *Bam*HI site in the CD-14B construct. Boxed regions show changes made to generate mutant C7. (**B**) Single or multiple base changes were introduced into the motif1-hairpin sequence of CD-14B as shown. Mismatch mutations are boxed, while compensatory mutations that restored the stability of the hairpin are shaded. The names of individual constructs are shown next to the mutations.

the entire motif1-hairpin *in vitro* suggests that the role of the motif1-hairpin may be similar in the *in vitro* 3′-TX system and the *in vivo* sat-RNA C–sat-RNA D recombination system.

Comparison of the effect of mutations within the motif1-hairpin and the upstream putative primer-binding region on 3′-TX and recombination in vivo

To characterize the sequence and structural requirements of the motif1-hairpin in 3′-TX and recombination *in vivo*, three types of mutations were introduced into the hairpin: (i) destabilizing mutations that changed the stability of the hairpin; (ii) compensatory mutations that restored base pairing within the stem; and (iii) mutations in single-stranded regions that did not change the stability of the hairpin predictably. In this assay, the template was CD-14B that contains sequences similar to CD-14mini and, in addition, a 147 nucleotide sequence representing the 5′ segment of sat-RNA C. CD-14B supported 3′-TX similarly to CD-14mini (data not shown).

Mutations in the motif1-hairpin of CD-14B are depicted in Figure 3B, and their effects on 3′-TX are shown in Table I. In addition, sat-RNA C containing the corresponding motif1-hairpin mutations were tested for *in vivo* RNA recombination with sat-RNA D in whole turnip plants. For these studies, the positive-stranded sat-RNA C-derived constructs contained a 22 nucleotide deletion near the 5′ end that required repair through recombination with sat-RNA D in order to obtain viable sat-RNA C progeny in co-infections with wild-type sat-RNA D and TCV helper virus (Cascone *et al.*, 1993).

Stem-destabilizing mutations U183G and U185G reduced 3′-TX to 12.3 and 6.8%, respectively, of the level obtained with CD-14B carrying the wild-type motif1-hairpin. In addition, these mutations eliminated detectable *in vivo* recombination between sat-RNA D and sat-RNA C (Table I). Compensatory mutations that restored the base pairing in the motif1-hairpin increased 3′-TX to 21.8 and 24.4% (U183G/A206C and U185G/A202C, respectively) and restored *in vivo* recombination to the wild-type level. Two other stem-destabilizing mutations (LStem/3G and A189U) that reduced 3′-TX to 23.5 and 22.9% were recombination incompetent *in vivo*. Three-base compensatory mutations in constructs LStem/3GC and UStem/3GC that preserved the stability of the motif1-hairpin resulted in 41.0 and 25.4% 3′-TX activity, respectively, and showed 12 and 17% recombination activity *in vivo*, respectively. Deletion of the three bases in the U-bulge reduced 3′-TX to 9.4% and eliminated recombination *in vivo* (ΔU3, Table I).

Single mismatch mutations within the loop region reduced 3′-TX and *in vivo* recombination to various extents (Table I). Mutants G191C, U192A, G194A and G195U generated 3′-TX products at 37.3–50.9% the level of CD-14B, while supporting *in vivo* recombination at 40–75% of the level of sat-RNA C with a wild-type motif1-hairpin. Among the loop mutants, those with point mutations at positions 193 and 196 (constructs C193U and U196C) inhibited both 3′-TX (22.0 and 27.7%, respectively) and *in vivo* recombination (non-detected) to the largest extent.

To characterize whether hybridization between sat-RNA D sequence and the region 3′ of the motif1-hairpin in sat-RNA C (schematically shown as the priming stem in Figure 1B) is required for 3′-TX, seven mismatch mutations that were predicted to destabilize a portion of the priming stem were introduced into CD-14B (Figure 3A). The resulting construct (C7) supported 3′-TX at only 9.9% of the level of wild-type CD-14B (Table I). The recombinogenic, deletion version of sat-RNA C with mutations corresponding to those of C7 supported recombination *in vivo* at only 18% of the level of the non-mutated sat-RNA C deletion derivative (Table I). These experiments demonstrated that sat-RNA C minus strand sequences 3′ of the hotspot region at the base of the motif1-hairpin influenced the frequency of recombination *in vivo* and the efficiency of 3′-TX *in vitro*.

To test whether the sat-RNA C recombinants with mutations within their motif1-hairpin were viable, full-length sat-RNA C constructs similar to the above *in vivo* tested constructs, but without the 22 nucleotide deletion, were generated and tested in whole turnip plants (for details, see Cascone *et al.*, 1993). All the tested full-length sat-RNA C constructs with mutations were viable (data not shown).

Table I. Mutations in the motif 1-hairpin and the priming stem influence 3′-TX

Template	Mutations	3′-TX activity[a]	*In vivo* recombination[b]
CD-14B	wild-type	100	100 (18/18)
Lower stem mutants			
LStem/3G	$_{207}$CCC$_{209}$→GGG	23.5 ± 3.7	0 (0/18)
LStem/3GC	$_{180}$GGG$_{182}$→CCC, $_{207}$CCC$_{209}$→GGG	41.0 ± 4.2	12 (2/17)
U183G	$_{183}$U→G	12.3 ± 1.7	0 (0/6)[c]
U183G/A206C	$_{183}$U→G, $_{206}$A→C	21.8 ± 2.2	100 (6/6)[c]
Bulge mutant			
ΔU3	Δ$_{203}$UUU$_{205}$	9.4 ± 3.0	0 (6/6)[c]
Upper stem mutants			
U185G	$_{185}$U→G	6.8 ± 1.8	0 (0/6)[c]
U185G/A202C	$_{185}$U→G, $_{202}$A→C	24.4 ± 1.4	100 (6/6)[c]
UStem/3GC	$_{186}$GGG$_{188}$→CCC, $_{199}$CCC$_{201}$→GGG	25.4 ± 3.6	17 (2/17)
A189U	$_{189}$A→U	22.9 ± 0.1	0 (0/6)[c]
Loop mutants			
G191C	$_{191}$G→C	37.3 ± 0.5	50 (6/12)
U192A	$_{192}$U→A	50.9 ± 3.6	40 (4/10)
C193U	$_{193}$C→U	22.0 ± 5.3	0 (0/6)[c]
G194A	$_{194}$G→A	38.8 ± 0.6	58 (7/12)
G195U	$_{195}$G→U	47.6 ± 21.4	75 (9/12)
U196C	$_{196}$U→C	27.7 ± 5.8	0 (0/12)
Priming stem mutants			
C7	$_{157}$CCGACA$_{162}$→AUAUAC, $_{164}$A→G	9.9 ± 3.6	18 (3/17)

[a]Average percentage and standard error of three independent 3′-TX analyses.
[b]Percentage of plants accumulating sat-RNA C–sat-RNA D recombinants. The number of plants with recombinants and the total number of plants inoculated are shown in parentheses.
[c]Data from Cascone *et al.* (1993).

The motif1-hairpin is an RdRp-binding site

The above studies demonstrate that the motif1-hairpin is required for high level 3′-TX. One possible role for the motif1-hairpin in 3′-TX is for recruitment of the RdRp. To test whether the motif1-hairpin is able to interact with the RdRp or if the priming stem is also required, a competition assay was performed. In this assay, the template was CD-27 that contains sequences similar to CD-27mini and, in addition, a 147 nucleotide sequence representing the 5′ segment of sat-RNA C (located 5′ of the motif1-hairpin, as shown in Figure 4). The competing RNAs were derived from a variant of CD-27mini that lacked the sat-RNA D sequence, eliminating the priming stem (Figure 4). The resulting Cmini series of constructs retained the wild-type motif1-hairpin (designated Cmini) or contained modifications in the motif1-hairpin.

Programing the RdRp reactions with a constant amount of template (CD-27) and increasing amounts of competing RNAs (2-, 10- and 40-fold the level of template) revealed that Cmini reduced 3′-TX of CD-27 by 7.3% when present in 2-fold excess, by 48.0% when in 10-fold excess, and by 83.8% when in 40-fold excess (Table II). Construct Cmini/mot1 with a partial truncation within the motif1-hairpin did not compete as efficiently as Cmini, reducing 3′-TX of CD-27 by 5.5, 11.7 and 26.9% when present in 2-, 10- and 40-fold excess, respectively (Table II). A derivative of Cmini with a single base alteration in the stem of the motif1-hairpin (designated Cmini/U183G) was also an inefficient competitor when compared with Cmini, reducing 3′-TX of CD-27 by 5.3, 21.2 and 36.1% when present in 2-, 10- and 40-fold excess. This result is consistent with the debilitating effect of U183G mutation on 3′-TX when present in CD-14B (see above). Addition of tRNA into the RdRp reaction in 5-, 10- and 40-fold excess, respectively, reduced 3′-TX of CD-27 by not more than 7% (Table II). Overall, these data demonstrate that Cmini RNA with the wild-type motif1-hairpin, but without the priming stem, can reduce 3′-TX on template RNA with the primer stem. Mutated or truncated derivatives of the motif1-hairpin and the unrelated tRNA did not compete efficiently with the 3′-TX of the template RNA. The simplest interpretation of these results is that the wild-type motif1-hairpin competes for the RdRp, thus making less RdRp available for the 3′-TX reaction.

Artificial priming stems support efficient 3′-TX

To test whether the sequence of the priming stem is important for efficient 3′-TX, the priming stem sequence was replaced with artificial sequences also capable of forming base-paired structures (Figure 5A). A 12 bp GC-rich stem and seven nucleotide loop (GC12mini) was 73% as efficient at 3′-TX as CD-27mini. The site of initiation was at the base of the GC-rich stem, based on S1 nuclease digestion followed by size determination on denaturing gels (Figure 5B). A 17 bp AU-rich priming stem with one bulged nucleotide and terminating with three C residues at the 3′ end and a seven nucleotide loop (AU/GCmini) was more efficient (129%) than CD-27mini in 3′-TX reactions. Constructs AU5mini and AU17mini containing only AU base-paired priming stems showed reduced 3′-TX activity (30.4 and 63.4%) when compared with CD-27mini (Figure 5A). The hairpin-like 3′-TX products for AU/GCmini, AU17mini and AU5mini migrated more slowly in 5% polyacrylamide–8 M urea gels, and S1 nuclease digestion revealed resistant RNA bands ~12 nucleotides shorter than that obtained with CD-27mini

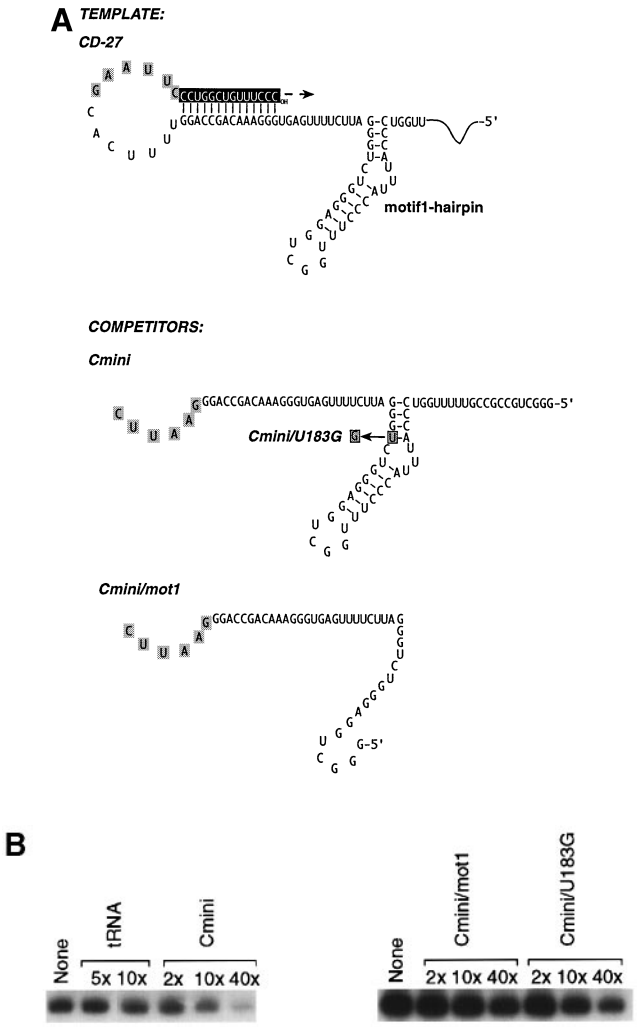

Fig. 4. Excess amounts of the motif1-hairpin inhibit 3′-TX. (**A**) Sequences and structures of the CD-27 template RNA and competitor RNAs that lack the priming stem. The competitor RNAs contain the wild-type motif1-hairpin (Cmini), have a stem-destabilizing U to G mutation (Cmini/U183G) or contain a 5′-truncated motif1-hairpin (Cmini/mot1). Shadings are as described in the legend to Figure 1. (**B**) A representative experiment showing denaturing gel analysis of radiolabeled 3′-TX products obtained using CD-27 as template. TCV RdRp preparations were programed with CD-27 template RNA and increasing amounts of the competitor RNAs (as described in Materials and methods) indicated above the lanes. The efficiency of 3′-TX on the CD-27 template RNA was measured as described in the legend to Figure 2. 'None' indicates that no competing RNA was added.

(Figure 5B). Although the exact sites of initiation were not determined for these constructs, the altered migration of the 3′-TX products for AU/GCmini, AU5mini and AU17mini when compared with CD-27mini and GC12mini is consistent with the high AU-rich content of the priming stem, which may not be base paired during electrophoresis. In addition, the AU-rich priming stem may be cleaved by the single strand-specific S1 nuclease due to 'breathing' within the less stable AU-rich region. Alternatively, the AU-rich sequences within the priming stem may misalign, causing aberrant migration and sensitivity to S1 nuclease.

To test whether the motif1-hairpin facilitates 3′-TX with the artificial priming stems, GC12mini/mot1 and AU/GCmini/mot1, which contained only the 3′ half of the motif1-hairpin and various priming stems, were constructed. The 3′-TX products for GC12mini/mot1 and AU/GCmini/mot1 were reduced by 30-fold from the level of GC12mini and AU/GCmini, respectively (Figure 2B), demonstrating that the priming stem alone cannot support efficient 3′-TX. These data demonstrate that there is no specific sequence requirement within the priming stem for 3′-TX in this system. The lack of sequence specificity within the priming stem suggests that the TCV RdRp does not recognize the priming stem but, instead, it recognizes the motif1-hairpin present on the template RNA.

Table II. Excess amount of motif1-hairpin reduces 3′-TX

Competitor		3′-TX activity[a]
None		100
tRNA	5×	97.9 ± 12.1
tRNA	10×	94.8 ± 1.8
tRNA	40×	93.1 ± 5.6
Cmini	2×	92.7 ± 5.2
Cmini	10×	52.0 ± 8.3
Cmini	40×	16.2 ± 1.8
Cmini/mot1	2×	94.5 ± 6.2
Cmini/mot1	10×	82.3 ± 6.2
Cmini/mot1	40×	73.1 ± 1.1
Cmini/U183G	2×	94.7 ± 5.3
Cmini/U183G	10×	78.8 ± 8.7
Cmini/U183G	40×	63.9 ± 10.5

[a]Average percentage and standard error of three independent 3′-TX analyses using CD-27 as template. See Figure 4 for a representative experiment.

Discussion

Understanding the mechanism of RNA recombination has been hampered by the lack of *in vitro* systems that allow direct visualization and characterization of recombination intermediates and end-products. The available *in vivo* and *in vitro* RNA recombination systems are inefficient; thus, characterizing the recombinants requires one or more amplification steps (Lai, 1992; Nagy and Bujarski, 1992; Chetverin *et al.*, 1997; Duggal *et al.*, 1997; Qiao *et al.*, 1997; Tang *et al.*, 1997). These post-recombination amplification steps, regardless of whether they are occurring *in vivo* or *in vitro*, have disadvantages, since they can favor amplification of some recombinants over others. For example, in most *in vivo* and *in vitro* systems (Banner and Lai, 1991; Jarvis and Kirkegaard, 1992; Nagy and Bujarski, 1992; Chetverin *et al.*, 1997; Tang *et al.*, 1997), only the viable or replication-competent recombinants can be detected. In addition, the sequence of some recombinants can be modified further by mutations, deletions and rearrangements during the amplification step. Altogether, amplification can lead to misrepresentation of some recombinants in the obtained 'recombinant pool', making difficult or even excluding the possibility of drawing conclusions about the mechanism of their generation. The amplification steps can also produce artifactual recombinants and those must be discriminated carefully from 'true' recombinants. Moreover, the requirement for amplification does not allow the direct examination of recombination intermediates whose structure would be important in unraveling the mechanism of RNA recombination.

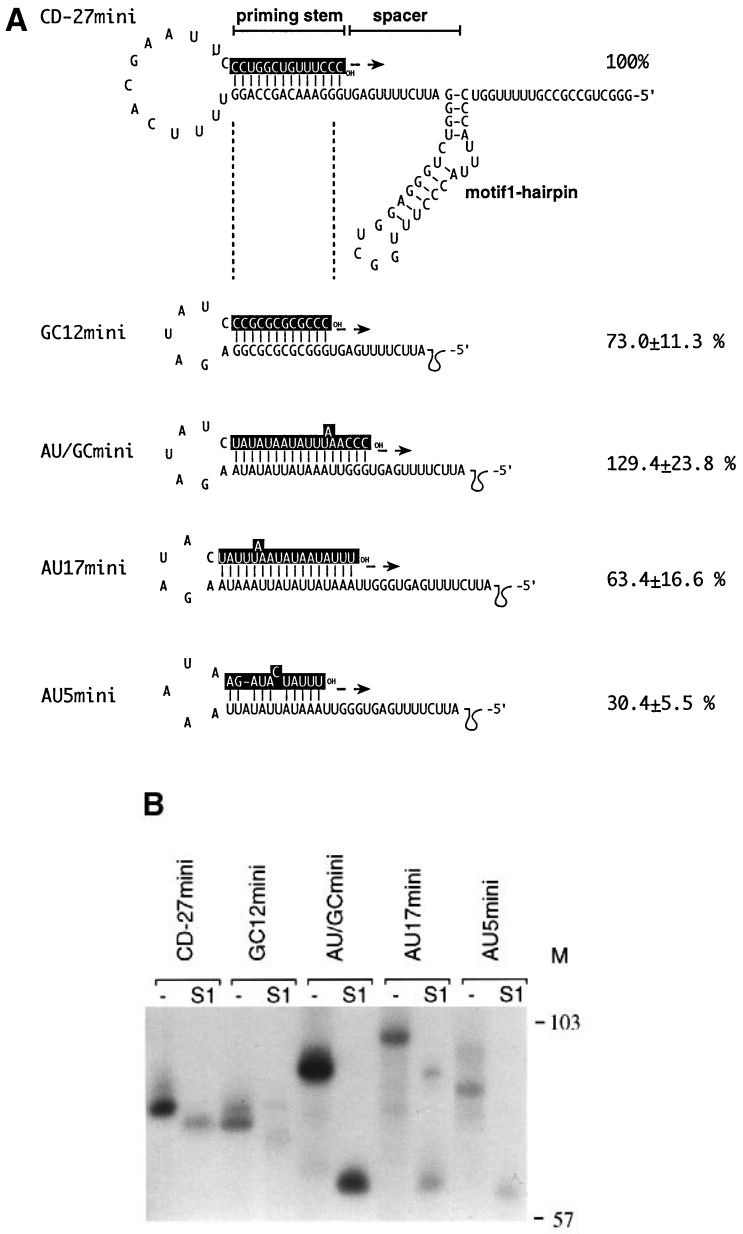

Fig. 5. Various priming stems can support 3′-TX. (**A**) Sequences and structures of the priming stems and spacer regions for the constructs indicated. The efficiency of 3′-TX on the template RNAs was measured as described in the legend to Figure 2. (**B**) Autoradiogram of denaturing PAGE of 3′-TX products. Lanes depicted by – and S1 denote products that were not treated, or treated by S1 nuclease, respectively. Note that in the untreated samples, the hairpin-like RNAs migrate aberrantly.

We have developed an *in vitro* TCV system that does not require amplification of RNA molecules. To avoid the need for amplification of the products, the *in vitro* system was optimized by favoring the interaction between putative RNA recombination intermediates by covalently linking the putative RNA intermediates with a short linker region. The sequence and structure of recombination intermediates were delineated from previous *in vivo* experiments that also resulted in a testable recombination model. This model predicted that RNA recombinants in the sat-RNA D–sat-RNA C system of TCV are formed by a replicase-mediated strand transfer mechanism where the nascent strand, made on the negative-stranded donor sat-RNA D by the replicase, serves as a primer during re-initiation of RNA synthesis on the negative-stranded sat-RNA C. According to the model, this process leads to a chimeric (recombinant) sat-RNA D–sat-RNA C molecule if a putative RdRp-binding sequence (termed the motif1-hairpin) is present on the acceptor sat-RNA C. The three-component primer extension reaction predicted to occur in infected cells *in vivo* during RNA recombination should be similar to a simplified two-component 3′-TX reaction *in vitro* if the correct intermediates are in proximity in the test tube. This prediction was supported by nearly all of the data presented herein. For example, the motif1-hairpin of sat-RNA C was required for sat-RNA D–sat-RNA C recombination *in vivo* (Cascone *et al.*, 1990, 1993; this work) and also greatly facilitated 3′-TX *in vitro*. Also, the junction sites of *in vivo* recombinants and the initiation of 3′-TX products *in vitro* were mapped to the same region on sat-RNA C, at or close to the base of the motif1-hairpin. In addition, minus strand sequences 3′ of the

motif1-hairpin of sat-RNA C greatly influenced the frequency of *in vivo* recombination (Cascone *et al.*, 1993; this work) and the efficiency of 3′-TX *in vitro*. These similarities between the *in vivo* and *in vitro* data give crucial support for the replicase-mediated template-switching model of recombination in TCV. In addition, the *in vitro* system allowed for defining RNA–RNA and protein–RNA interactions that probably influence template-switching events *in vivo* as well (see below).

In spite of the above similarities between the *in vitro* 3′-TX and *in vivo* recombination systems, there were exceptions that should be noted. When compared with the corresponding hairpin-destabilizing mutants, mutants with compensatory mutations in the motif1-hairpin (U183G/A206C and U185G/A202C, Table I) restored the efficiency of 3′-TX only partially, while restoring the efficiency of *in vivo* recombination to the wild-type level. It is possible that the mutated motif1-hairpin has a slightly different structure *in vitro* than *in vivo*. The other difference between the *in vitro* 3′-TX and the *in vivo* recombination systems was that the latter can be abolished completely by mutations within the motif1-hairpin, while 3′-TX can only be reduced to a low level, but cannot be abolished. This 'background' level of 3′-TX may be the consequence of inefficient interaction between the RdRp and the template RNA in the two-component 3′-TX system, while the possibility for interaction is reduced below the level of detection in the three-component *in vivo* recombination system. The amount of primer RNA (the aborted nascent sat-RNA strands) is not known *in vivo*, but is probably less than in the *in vitro* 3′-TX reaction. In addition, the rate of amplification or the stability of the *de novo* sat-RNA C–sat-RNA D recombinants can be influenced by the motif1-hairpin mutations in the *in vivo* recombination system, but not in our *in vitro* system where there is no amplification step and the RdRp products are stable hairpin-like RNAs. Other possible explanations include loss of a component by the RdRp preparations resulting in lower specificity *in vitro*. Finally, in the replicase-driven, strand-switching model, it is not clear whether the nascent strand together with the RdRp simply falls off the donor template and is then available for capture by the acceptor, or if the acceptor can assist in removing (i.e. can displace) the nascent strand and the RdRp from the donor. If the latter, one might expect the *in vivo* situation to have more stringent requirements, because the *in vitro* system only tests the former.

The use of an *in vitro* system made possible the identification of two RNA elements that can influence 3′-TX and, analogously, RNA recombination in TCV and its associated RNAs. The first RNA element required for the 3′-TX is the motif1-hairpin. Mutagenesis experiments revealed that both the sequence and the secondary structure of the motif1-hairpin can influence 3′-TX and *in vivo* recombination. Stem-destabilizing mutations in both the lower and upper stems reduced 3′-TX greatly and eliminated *in vivo* recombination. Compensatory mutations that restored the stability of the hairpin increased 3′-TX by 2- to 3-fold and partially restored or, for some mutants, completely restored *in vivo* recombination. Mutations within the loop region reduced both 3′-TX and *in vivo* recombination. Further studies will address whether there is base-specific contact(s) between the motif1-hairpin sequence and the RdRp during 3′-TX.

Competition studies revealed that the wild-type motif1-hairpin can compete more efficiently with the 3′-TX of the CD-27 template than either a mutated or truncated derivative or the unrelated tRNA, suggesting that the TCV RdRp probably recognizes this element. The proposed binding of motif1-hairpin to the RdRp, however, is not strong or stable, since a 10-fold excess of competing RNA was required to produce a 50% reduction in 3′-TX. It is possible that the priming stem stabilizes RdRp binding to the motif1-hairpin. Alternatively, RNA synthesis (due to the 3′-TX) keeps the RdRp on the CD-27 template RNA for a longer period than the 'non-productive' binding to the competing RNAs that have less efficient 3′-TX due to the lack of a priming stem. The above experiments also demonstrated that the motif1-hairpin is not a promoter element in the strict sense, since no efficient *de novo* initiation was detected in the absence of the natural RdRp promoters. Accordingly, we propose that the motif1-hairpin is important in recruiting the RdRp, and the complex supports efficient 3′-TX only if the appropriate priming stem is available.

The second RNA element required for the 3′-TX is the priming stem that is formed by base pairing between the 3′ end of the RNA templates and an internal sequence 3′ of the motif1-hairpin. Mutations that destabilized the priming stem (C7, Table I) or eliminated it by removing 3′-end sequence (data not shown) reduced the efficiency of 3′-TX. The reduced level of 3′-TX obtained with the above constructs was not due to changes in the primary RNA sequences, since several templates with different artificial sequences capable of priming stem formation supported efficient 3′-TX (Figure 5A). Analogously to the requirement for the priming stem for efficient 3′-TX, the requirement for RNA–RNA interaction is also supported by data obtained for RNA recombination *in vivo* between sat-RNA C and sat-RNA D, since extensive mutations (e.g. C7, Table I) and deletions (Cascone *et al.*, 1993) 3′ of the motif1-hairpin on negative strands of sat-RNA C reduced the efficiency of recombination. It is important to note, however, that stable priming stems alone supported only very inefficient 3′-TX, arguing that the recognition of the priming stem by the TCV RdRp in the absence of the motif1-hairpin is inefficient.

As stated above, many different sequences in the priming stem can be used efficiently by the TCV RdRp if they preserve the stability of the stem. Interestingly, templates with priming stems that contained both GC and AU nucleotides were more active in 3′-TX than AU- or GC-rich sequences alone. Also, a 10 bp primer stem with two bulged nucleotides (AU5mini) was sufficient to support higher than background levels of 3′-TX. The role of short base-paired regions in promoting recombination has also been proposed for many recombination systems, including noda- (Li and Ball, 1993), bromo- (Nagy and Bujarski, 1995), tombusviruses (White and Morris, 1995), Qβ (Biebricher and Luce, 1992) and Φ6 bacteriophages (Onodera *et al.*, 1993). In addition, sequences that contained both GC and AU nucleotides were favored for homologous recombination in BMV where RNA–RNA interaction, similar to the above priming stem in the chimeric sat-RNA D–sat-RNA C constructs, during the

landing of the nascent strand on the acceptor strand has been proposed (Nagy and Bujarski, 1997).

The priming stem in the absence of the motif1-hairpin cannot drive efficient 3′-TX with the TCV RdRp. Thus, the TCV RdRp, which is naturally promoter dependent and capable of *de novo* initiation (Song and Simon, 1994, 1995), is different from most of the DNA-dependent DNA polymerases, reverse transcriptases and T7 DNA-dependent RNA polymerase (Konarska and Sharp, 1989; Cazenave and Uhlenbeck, 1994) that only require base pairing of the very 3′-end bases between the primer and the template for strand elongation. In contrast, the promoter-dependent RdRps may require or favor the proximity of a promoter or promoter-like element in order to use primers efficiently. For example, both BMV and TCV RdRps were capable of primer elongation from their 3′-terminal negative strand initiation promoters, but they were incapable of primer elongation from primers hybridizing randomly at internal positions (Kao and Sun, 1996; Nagy *et al.*, 1997). Also, the influenza virus and Thogoto virus RdRps can only initiate mRNA synthesis from their 3′-terminal promoters using dinucleotide or oligonucleotide primers, but not from internal sites (Seong and Brownlee, 1992; Leahy *et al.*, 1997). Base pairing between the primers and the template is not absolutely required in the Thogoto virus system, but influences the efficiency and site of initiation (Leahy *et al.*, 1997). Another example of promoter-dependent priming at the 3′ end of plus strands has been proposed for poliovirus (Harris *et al.*, 1994). This model predicts that a protein cleavage product, termed Vpg, is uridylylated and then used to initiate minus strand synthesis by the poliovirus RdRp complex bound to the 3′-terminal promoter. In contrast to the multisubunit RdRps, the polymerase subunit of the poliovirus and the related hepatitis C virus RdRps are capable of non-sequence-specific primer extensions regardless of the presence of promoter sequences (Neufeld *et al.*, 1991; Behrens *et al.*, 1996). The leader-primed RNA transcription in coronaviruses requires both short sequence complementarity between the primer and the template and the presence of a putative RdRp-binding sequence on the template RNA (Baker and Lai, 1990; Zhang and Lai, 1995). In addition, the reverse transcriptase of the Mauriceville plasmid, which normally initiates DNA synthesis *de novo* at its 3′-terminal promoter, is capable of primer extension from its 3′-terminal promoter, even if the primer is not base paired with the template (Wang and Lambowitz, 1993). Similarly to the above RdRps, the reverse transcriptase of the Mauriceville plasmid cannot efficiently use primers hybridizing randomly at internal positions (Chen and Lambowitz, 1997). All these data suggest that primer-initiated strand elongation by a promoter-dependent RdRp or reverse transcriptase of the Mauriceville plasmid may be facilitated by a proximal promoter or promoter-like element. This is a novel phenomenon that may be characteristic of several promoter-dependent RdRps.

The finding that an RdRp-binding element facilitates *in vitro* 3′-TX and *in vivo* RNA recombination in TCV may have implications for other viral systems as well. For example, subgenomic RNA promoters or related sequences that bind their corresponding RdRp frequently are found as recombination sites in BMV (Allison *et al.*, 1990), Sindbis virus (Weiss and Schlesinger, 1991) and tobacco mosaic virus (Beck and Dawson, 1990). Subgenomic RNA promoter-like elements may also have played a role in reshuffling functional ‘modules’ and in inter(intra-)viral recombination that facilitated viral evolution (Gibbs, 1987; Allison *et al.*, 1989; Miller *et al.*, 1995). In addition, many crossover events in BMV (Nagy and Bujarski, 1992; Rao and Hall, 1993), Sindbis virus (Hajjou *et al.*, 1996), tobraviruses (Goulden *et al.*, 1991), cucumoviruses (Fernandez-Cuartero *et al.*, 1994), alfalfa mosaic virus (Huisman *et al.*, 1989) and barley stripe mosaic virus (Edwards *et al.*, 1992) are located within 3′- or 5′-terminal promoter sequences. These promoter sequences, similarly to the subgenomic promoters, may have played a role in recombination events by recruiting the RdRp–nascent strand complex.

Materials and methods

RNA template construction

For the *in vivo* recombination studies, a derivative of the full-length, biologically active cDNA construct of sat-RNA C (pCAMD, Cascone *et al.*, 1993) that contained *Apa*I and *Mlu*I sites at positions 206 and 142, respectively, combined with a 22 base, 5′-proximal deletion between positions 57 and 78 was mutagenized using the method of Kunkel (1985) with a partially degenerate primer (5′-CCCAGACCCtccagccaaa-GGGTAAATGGG-3′, where the lower case letters represent degenerate bases at a ratio of 95% wild-type to 1.66% each of the other three bases) to obtain G191C, U192A, G194A, G195U and U196C, respectively. Similarly, the pCAMD versions of UStem/3GC, LStem/3G, LStem/3GC, ΔU3 and C7 were generated with primers CXexgcL (5′-ATCCCA-GAGGGTCCAGCCAAACCCTAAATGGGC-3′, where the mutated bases are underlined), CX180–182 (5′-TCAAAAGAATGGGAGAC-CCT-3′), CX208–210 (5′-AAGGGTAAATCCCCCCAAAAACG-3′), CXdB (5′-CAGCCAAAGGGTΔΔΔTGGGCCCAA-3′, where the deleted bases are marked with Δ) and CX46 (5′-GACGCGTGAAAAC-ctggctgtttcccactcaaaaGAATCCCAGACC-3′), respectively. Mutants were identified by dideoxy sequencing using Sequenase (Amersham). The purified DNA representing each construct was linearized with *Eco*RI prior to *Escherichia coli* RNA polymerase transcription (Cascone *et al.*, 1990).

For the *in vitro* 3′-TX experiments, RNA templates were obtained by *in vitro* transcription with T7 RNA polymerase using either PCR-amplified DNA templates or purified and linearized plasmid DNA (Song and Simon, 1994; Nagy *et al.*, 1997). After phenol/chloroform extraction, unincorporated nucleotides were removed by repeated ammonium acetate/isopropanol precipitation (Song and Simon, 1994; Nagy *et al.*, 1997). The obtained RNA transcripts were dissolved in sterile water and their amount and size were measured by a UV spectrophotometer and 5% polyacrylamide–8 M urea gel (denaturing PAGE) analysis (Song and Simon, 1994; Nagy *et al.*, 1997).

CD-27 DNA was obtained with two sequential rounds of PCR, first using primers hairpin-1 [5′-GGG(A/T)(A/T)(A/T)(C/T)AGCCAGGG-AATTCGTGAAAACCTGGCTG-3′] and T7C3′ (5′-GTAATACGACT-CACTATAGGGCAGGCCCCCCG-3′), and pT7C(+) template (Song and Simon, 1994) that contains the full-length cDNA of sat-RNA C, followed by gel purification of the PCR product and a second round of PCR with primers har1/0 (5′-GGGAAACAGCCAGGGAATTCGTGA-3′) and T7C3′. CD-27mini DNA was also obtained by PCR with primers har1/0 and T7motif1 (5′-GTAATACGACTCACTATAGGGCTGCCG-CCGTTTTTGG-3′) using CD-27 as template. CD-13mini DNA was generated by PCR using primer pairs CD-13 (5′-GGACTCTTTCG-AGTGGGATACTGCCAGGGAATTCGTGA-3′) and T7motif1, while CD-14mini DNA was obtained with primer pairs SatD/hinc (5′-GTCG-ACTCTTTCGAGTGG-3′) and T7motif1 using CD-13mini as template, followed by cloning to the *Sma*I site of pUC19 and cleavage with *Hin*cII.

Constructs AU/GCmini, GC12mini and AU17mini were obtained by PCR with primers Har-AU (5′-GGGTTTAAATATTATATAGATATCTT-ATATAATATTTAACCCACTCAAAAGAATC-3′), Har-GC (5′-GGGC-GCGCGCGGTGATATCTCCGCGCGCGCCCACTCAAAAGAATC-3′) and AU-17 (5′-AAATATTATATTTAAATAGTATCTTATTTAATATA-ATATTTAACCCACT-3′), respectively, in combination with primer T7motif1 using CD-27 as template. Construct AU5mini was obtained by digesting AU17mini with *Dra*I, followed by agarose gel purification

of the cleaved product. Constructs CD-27mini/mot1, GC12mini/mot1 and AU/GCmini/mot1 were generated by PCR with primers T7motif1-short (5′-GTAATACGACTCACTATAGGGCTGGAGGGTC-3′) and either Har1/0, Har-GC or Har-AU using CD-27, GC12mini and AU/GCmini, respectively, as templates.

CD-14B was generated by cloning the PCR product obtained using pT7C(+) DNA template with primers T7C3′ and hairpin-satD [5′-GGG(A/T)(A/T)CCTTTCGAGTGGGATACTGCCAGGATATCGTAC-GGGAGCGTG-3′], into the *Sma*I site of pUC19. Two mutations were engineered into the priming stem of construct CD-14B that created a *Bam*HI restriction site at the 3′ end of the cDNA construct while maintaining the base pairing in the priming stem in the derived transcript. In addition, a unique *Eco*RV sequence was engineered into the loop region. The template DNA for T7 RNA polymerase transcription was linearized by *Bam*HI cleavage. Derivatives of CD-14B with mutations in the motif1-hairpin or the priming stem, such as LStem/3G, LStem/3GC, U183G, U183G/A206C, U185G, U185G/A202C, ΔU3, UStem/3GC, A189U, G191C, U192A, C193U, G194A, G195U, U196C and C7, were generated by PCR with primers T7C3′ and hairpin-satD using the corresponding pCAMD-derived templates described above and in Cascone *et al.* (1993). The PCR-amplified DNA corresponding to each of the above constructs was cloned, linearized with *Bam*HI and transcribed as described for CD-14B above. Sequence analysis of the obtained clones confirmed the presence of only the desired modifications.

Constructs Cmini and Cmini/mot1 were generated by PCR with the same 3′ primer (Har1PCR, 5′-GAATTCCCTGGCTGTTTCCC-3′) and one of the 5′ primers, T7motif1 or T7motif1-short, respectively, using CD-27 as template. Cmini/U183G was constructed with the method used for Cmini, except that U183G served as the PCR template.

3′-TX product analysis

Preparation of template-dependent RdRp from TCV-infected turnip plants, *in vitro* 3′-TX reactions (similar to transcription reactions, but using different RNA templates) and product analysis were carried out as previously described (Nagy *et al.*, 1997) using a total of 20 μl of RdRp reaction mixture that contained 3 μg of template RNA. For the competition studies, 1 μg of CD-27 template RNA and increasing amounts of competitor RNA (as shown in Figure 4) were used in a 30 μl RdRp reaction mixture.

3′-TX products were treated with S1 nuclease or RNase H in the presence of 1 μg of loop1 oligo (5′-AATTCGTGAAAA-3′, complementary to the loop region of CD-27, see Figure 1C) as described (Song and Simon, 1994, 1995) at 37°C for 1 h. After phenol/chloroform extraction and ammonium acetate/isopropanol precipitation, the products were analyzed on a 20 cm-long denaturing 5% polyacrylamide–8 M urea gel, followed by autoradiography and densitometry (Nagy *et al.*, 1997). The data were normalized based on the amount of template-directed radioactive UTP incorporated into the 3′-TX products and the molar amount of the template RNA in the RdRp reaction. For some experiments, the gels were stained with ethidium bromide, photographed and dried, followed by analysis with a phosphorimager as described (Nagy *et al.*, 1997).

The radioactively labeled 3′-TX product of CD-27 obtained from a 200 μl RdRp reaction was gel purified, then hybridized with loop1 oligo followed by digestion with RNase H as described above. The RNase H-cleaved product was gel purified and subjected to reverse transcription (RT) PCR with primer T7C3′ and MMLV reverse transcriptase (Song and Simon, 1995). Oligodeoxynucleotides T7C3′ and Har1PCR (5′-GAATTCCCTGGCTGTTTCCC-3′) were used for PCR. The ~210 base long PCR product was gel purified, cloned into the *Sma*I site of pUC19, and then sequenced using standard procedures (Sambrook *et al.*, 1989).

Detection of RNA recombination between sat-RNA C and sat-RNA D in whole plants

Turnip plants were inoculated with a mixture of sat-RNA C (CAMD series, see above), wild-type sat-RNA D and helper TCV RNA, as described previously (Cascone *et al.*, 1993). To test for the viability of sat-RNA C constructs, full-length sat-RNA C that contained mutations in the motif1-hairpin, but without the 22 nucleotide deletion (present in the CAMD series), were used for inoculation as descibed by Cascone *et al.* (1993). Total RNA isolation, Northern blot and RT–PCR analysis of sat-RNA C progeny were done according to a published procedure (Cascone *et al.*, 1993).

Acknowledgements

We thank Drs Clifford D.Carpenter and Judit Pogany for critical reading of the manuscript. This work was supported by National Science Foundation grants MCB-9419303 and MCB-9630191 to A.E.S.

References

Allison,R.F., Janda,M. and Ahlquist,P. (1989) Sequence of cowpea chlorotic mottle virus RNA2 and RNA3 and evidence of a recombination event during bromovirus evolution. *Virology*, **172**, 321–330.

Allison,R.F., Thompson,G. and Ahlquist,P. (1990) Regeneration of a functional RNA virus genome by recombination between deletion mutants and requirement for cowpea chlorotic mottle virus 3a and coat genes for systemic infection. *Proc. Natl Acad. Sci. USA*, **87**, 1820–1824.

Baker,S.C. and Lai,M.M.C. (1990) An *in vitro* system for the leader-primed transcription of coronavirus mRNAs. *EMBO J.*, **9**, 4173–4179.

Beck,D.L. and Dawson,W.O. (1990) Deletion of repeated sequences from tobacco mosaic virus mutants with two coat protein genes. *Virology*, **177**, 462–469.

Banner,L.R. and Lai,M.M.C. (1991) Random nature of coronavirus recombination in the absence of selection pressure. *Virology*, **185**, 441–445.

Behrens,S.-E., Tomei,L. and De Francesco,R. (1996) Identification and properties of the RNA-dependent RNA polymerase of hepatitis C virus. *EMBO J.*, **15**, 12–22.

Biebricher,C.K. and Luce,R. (1992) *In vitro* recombination and terminal elongation of RNA by Qβ replicase. *EMBO J.*, **11**, 5129–5135.

Carpenter,C.D., Oh,J.-W., Zhang,C. and Simon,A.E. (1995) Involvement of a stem–loop structure in the location of junction sites in viral RNA recombination. *J. Mol. Biol.*, **245**, 608–622.

Cascone,P.J., Carpenter,C.D., Li,X.H. and Simon,A.E. (1990) Recombination between satellite RNAs of turnip crinkle virus. *EMBO J.*, **9**, 1709–1715.

Cascone,P.J., Haydar,T.F. and Simon,A.E. (1993) Sequences and structures required for recombination between virus-associated RNAs. *Science*, **260**, 801–805.

Cazenave,C. and Uhlenbeck,O.C. (1994) RNA template-directed RNA synthesis by T7 RNA polymerase. *Proc. Natl Acad. Sci. USA*, **91**, 6972–6976.

Chen,B. and Lambowitz,A.M. (1997) *De novo* and DNA primer-mediated initiation of cDNA synthesis by the Mauriceville retroplasmid reverse transcriptase involve recognition of a 3′ CCA sequence. *J. Mol. Biol.*, **271**, 311–332.

Chetverin,A.B., Chetverina,H.V., Demidenko,A.A. and Ugarov,V.I. (1997) Nonhomologous RNA recombination in a cell-free system: evidence for a transesterification mechanism guided by the secondary structure. *Cell*, **88**, 503–513.

Dolja,V.V. and Carrington,J.C. (1992) Evolution of positive-strand RNA viruses. *Semin. Virol.*, **3**, 315–326.

Duggal,R., Cuconati,A., Gromeier,M. and Wimmer,E. (1997) Genetic recombination of poliovirus in a cell-free system. *Proc. Natl Acad. Sci. USA*, **94**, 13786–13791.

Edwards,M.C., Petty,I.T.D. and Jackson,A.O. (1992) RNA recombination in the genome of barley stripe mosaic virus. *Virology*, **189**, 389–392.

Fernandez-Cuartero,B., Burgyan,J., Aranda,M.A., Salanki,K., Moriones,E. and Garcia-Arenal,F. (1994) Increase in the relative fitness of a plant virus RNA associated with its recombinant nature. *Virology*, **203**, 373–377.

Figlerowitz,M., Nagy,P.D. and Bujarski,J.J. (1997) A mutation in the putative RNA polymerase gene inhibits nonhomologous, but not homologous, genetic recombination in an RNA virus. *Proc. Natl Acad. Sci. USA*, **94**, 2073–2078.

Gibbs,A. (1987) A molecular evolution of viruses: 'trees', 'clocks', and 'modules'. *J. Cell Sci.* (suppl.), **7**, 319–337.

Goulden,M.G., Lomonossoff,G.P., Wood,K.R. and Davies,J.W. (1991) A model for the generation of tobacco rattle virus (TRV) anomalous isolates: pea early browning virus RNA2 acquires TRV sequences from both RNA-1 and RNA-2. *J. Gen. Virol.*, **72**, 1751–1754.

Greene,A.E. and Allison,R.F. (1994) Recombination between viral RNA and transgenic plant transcripts. *Science*, **263**, 1423–1425.

Guan,H., Song,C. and Simon,A.E. (1997) RNA promoters located on (–)-strands of a subviral RNA associated with turnip crinkle virus. *RNA*, **3**, 1401–1412.

Hajjou,M., Hill,K.R., Subramaniam,S.V., Hu,J.Y. and Raju,R. (1996) Nonhomologous RNA–RNA recombination events at the 3′ nontranslated region of the Sindbis virus genome: hot spots and utilization of nonviral sequences. *J. Virol.*, **70**, 5153–5164.

Harris,K.S., Xiang,W., Alexander,L., Lane,W.S., Paul,A.V. and Wimmer,E. (1994) Interaction of poliovirus polypeptide 3Cdpro with

the 5′ and 3′ termini of the poliovirus genome. *J. Biol. Chem*., **269**, 27004–27014.
Huisman,M.J., Cornelissen,B.J.C., Groenendijk,C.F.M., Bol,J.F. and Van Vloten-Doting,L. (1989) Alfalfa mosaic virus temperature-sensitive mutants V. The nucleotide sequence of TBTS 7 RNA 3 shows limited nucleotide changes and evidence for heterologous recombination. *Virology*, **171**, 409–416.
Jarvis,T.C. and Kirkegaard,K. (1991) The polymerase in its labyrinth: mechanisms and implications of RNA recombination. *Trends Genet*., **7**, 186–191.
Jarvis,T.C. and Kirkegaard,K. (1992) Poliovirus RNA recombination: mechanistic studies in the absence of selection. *EMBO J*., **11**, 3135–3145.
Kao,C.C. and Sun,J.-H. (1996) Initiation of minus-strand RNA synthesis by the brome mosaic virus RNA-dependent RNA polymerase: use of oligoribonucleotide primers. *J. Virol*., **70**, 6826–6830.
King,A.M.Q. (1988) Genetic recombination in positive strand RNA viruses. In Domingo,E., Holland,J.J. and Ahlquist,P. (eds), *RNA Genetics.* CRC Press, Boca Raton, FL, Vol. II, pp. 149–185.
Kirkegaard,K. and Baltimore,D. (1986) The mechanism of RNA recombination in poliovirus. *Cell*, **47**, 433–443.
Konarska,M. and Sharp,P.A. (1989) Replication of RNA by the DNA-dependent RNA polymerase of phage T7. *Cell*, **57**, 423–431.
Kunkel,T.A. (1985) Rapid and efficient site-specific mutagenesis without phenotypic selection. *Proc. Natl Acad. Sci. USA*, **82**, 488–492.
Lai,M.C.M. (1992) RNA recombination in animal and plant viruses. *Microbiol. Rev.*, **56**, 61–79.
Leahy,M.B., Dessens,J.T. and Nuttall,P.A. (1997) *In vitro* polymerase activity of Thogoto virus: evidence for a unique cap-snatching mechanism in a tick-borne Orthomyxovirus. *J. Virol*., **71**, 8347–8351.
Li,Y. and Ball,L.A. (1993) Nonhomologous RNA recombination during negative-strand synthesis of flock house virus RNA. *J. Virol*., **67**, 3854–3860.
Miller,W.A., Dinesh-Kumar,S.P. and Paul,C.P. (1995) Luteovirus gene expression. *Crit. Rev. Plant Sci*., **14**, 179–211.
Nagy,P.D. and Bujarski,J.J. (1992) Genetic recombination in brome mosaic virus: effect of sequence and replication of RNA on accumulation of recombinants. *J. Virol*., **66**, 6824–6828.
Nagy,P.D. and Bujarski,J.J. (1993) Targeting the site of RNA–RNA recombination in brome mosaic virus with antisense sequences. *Proc. Natl Acad. Sci. USA*, **90**, 6390–6394.
Nagy,P.D. and Bujarski,J.J. (1995) Efficient system of homologous RNA recombination in brome mosaic virus: sequence and structure requirements and accuracy of crossovers. *J. Virol.*, **69**, 131–140.
Nagy,P.D. and Bujarski,J.J. (1996) Homologous RNA recombination in brome mosaic virus: AU-rich sequences decrease the accuracy of crossovers. *J. Virol.*, **70**, 415–426.
Nagy,P.D. and Bujarski,J.J. (1997) Engineering of homologous recombination hotspots with AU-rich sequences in brome mosaic virus: AU-rich sequences decrease the accuracy of crossovers. *J. Virol*., **71**, 3799–3810.
Nagy,P.D. and Simon,A.E. (1997) New insights into the mechanisms of RNA recombination. *Virology*, **235**, 1–9.
Nagy,P.D., Dzianott,A., Ahlquist,P. and Bujarski,J.J. (1995) Mutations in the helicase-like domain of protein 1a alter the sites of RNA–RNA recombination in brome mosaic virus. *J. Virol*., **69**, 2547–2556.
Nagy,P.D., Carpenter,C.D. and Simon,A.E. (1997) A novel 3′-end repair mechanism in an RNA virus. *Proc. Natl Acad. Sci. USA*, **94**, 1113–1118**.**
Neufeld,K.L., Richards,O.C. and Ehrenfeld,E. (1991) Purification, characterization, and comparison of poliovirus RNA polymerase from native and recombinant sources. *J. Biol. Chem*., **266**, 24212–24219.
Onodera,S., Qiao,X., Gottlieb,P., Strassman,J., Frilander,M. and Mindich,L. (1993) RNA structure and heterologous recombination in the double-stranded RNA bacteriophage φ6. *J. Virol*., **67**, 4914–4922.
Qiao,X., Qiao,J. and Mindich,L. (1997) An *in vitro* system for investigation of heterologous RNA recombination. *Virology*, **227**, 103–110.
Rao,A.L.N. and Hall,T.C. (1993) Recombination and polymerase error facilitate restoration of infectivity in brome mosaic virus. *J. Virol.*, **67**, 969–979.
Sambrook,J., Fritsch,E.F. and Maniatis,T. (1989) *Molecular Cloning: A Laboratory Manual*. 2nd edn. Cold Spring Harbor Laboratory Press, Cold Spring Harbor, NY.
Seong,B.L. and Brownlee,G.G. (1992) A new method for reconstituting influenza polymerase and RNA *in vitro*: a study of the promoter elements for cRNA and vRNA synthesis *in vitro* and viral rescue *in vivo*. *Virology*, **186**, 247–260.
Simon,A.E. and Bujarski,J.J. (1994) RNA–RNA recombination and evolution in virus infected plants. *Annu. Rev. Phythopathol*., **32**, 337–362.
Simon,A.E. and Howell,S.H. (1986) The virulent satellite RNA of turnip crinkle virus has a major domain homologous to the 3′ end of the helper virus genome. *EMBO J*., **5**, 3423–3428.
Simon,A.E. and Nagy,P.D. (1996) RNA recombination in turnip crinkle virus: its role in formation of chimeric RNAs, multimers, and in 3′-end repair. *Semin. Virol*., **7**, 373–379.
Song,C. and Simon,A.E. (1994) RNA-dependent RNA polymerase from plants infected with turnip crinkle virus can transcribe (+) and (–)-strands of virus-associated RNAs. *Proc. Natl Acad. Sci. USA*, **91**, 8792–8796.
Song,C. and Simon,A.E. (1995) Synthesis of novel products *in vitro* by an RNA-dependent RNA polymerase. *J. Virol*., **69**, 4020–4028.
Strauss,J.H. and Strauss,E.G. (1988) Evolution of RNA viruses. *Annu. Rev. Microbiol.*, **42**, 657–683.
Tang,R.S., Barton,D.J., Flanegan,J.B. and Kirkegaard,K. (1997) Poliovirus RNA recombination in cell-free extracts. *RNA*, **3**, 624–633.
Wang,H. and Lambowitz,A.M. (1993) The Mauriceville plasmid reverse transcriptase can initiate cDNA synthesis *de novo* and may be related to reverse transcriptase and DNA polymerase progenitor. *Cell*, **75**, 1071–1081.
Weiss,B.G. and Schlesinger,S. (1991) Recombination between Sindbis virus RNAs. *J. Virol.*, **65**, 4017–4025.
White,K.A. and Morris,T.J. (1995) RNA determinants of junction site selection in RNA virus recombinants and defective interfering RNAs. *RNA*, **1**, 1029–1040.
Zhang,X. and Lai,M.M.C. (1995) Interactions between the cytoplasmic proteins and the intergenic (promoter) sequence of mouse hepatitis virus RNA: correlation with the amounts of subgenomic RNAs transcribed. *J. Virol*., **69**, 1637–1644.
Zimmern,D. (1988) Evolution of RNA viruses. In Holland,J.J., Domingo,E. and Ahlquist,P. (eds), *RNA Genetics*. CRC Press, Boca Raton, FL, Vol. II, pp. 211–240.

Received January 2, 1998; revised and accepted February 16, 1998